Title 論文題目	Intravenous Infusion of Mesenchymal Stem Cells Promotes the Survival of Random pattern Flap in Rats （骨髄間葉系幹細胞の静脈投与による乱走皮弁の生存域の拡大）
Author(s) 著者	中川, 嗣文
Degree number 学位記番号	甲第3155号
Degree name 学位の種別	博士(医学)
Issue Date 学位取得年月日	2022-03-31
Original Article 原著論文	Plast Reconstr Surg. 2021 Oct 1;148(4):799-807
Doc URL	
DOI	10.1097/PRS.0000000000008327
Resource Version	Author Edition

EXPERIMENTAL

Intravenous Infusion of Mesenchymal Stem Cells Promotes the Survival of Random Pattern Flap in Rats

Running Head: Infused MSCs promote skin flap survival

Tsugufumi Nakagawa, M.D. [1, 2]; Masanori Sasaki, M.D. [1, 4, 5]; Yuko Kataoka-Sasaki, M.D. [4]; Takatoshi Yotsuyanagi, M.D. [2]; Christine Radtke, M.D. [3]; Jeffery D. Kocsis, Ph.D. [4, 5], Osamu Honmou, M.D. [1, 4, 5]

[1] Department of Neural Regenerative Medicine, Research Institute for Frontier Medicine, Sapporo Medical University School of Medicine, Sapporo, 060-8556, Japan

[2] Department of Plastic and Reconstructive Surgery, Sapporo Medical University School of Medicine, Sapporo, Hokkaido, 060-8556, Japan

[3] Department of Plastic and Reconstructive Surgery, Medical University of Vienna, Währinger Gürtel 18–20, 1090, Vienna, Austria

[4] Department of Neurology, Yale University School of Medicine, New Haven, Connecticut, 06510, USA

[5] Center for Neuroscience and Regeneration Research, VA Connecticut Healthcare System, West Haven, Connecticut, 06516, USA

Corresponding Author:

Masanori Sasaki M.D.

Department of Neural Regenerative Medicine, Research Institute for Frontier Medicine,

Sapporo Medical University School of Medicine,

Sapporo, Hokkaido, 060-8556, Japan

E-mail: msasaki@sapmed.ac.jp

Financial Disclosure Statement:

None of the authors has a financial interest to declare regarding the content of this work.

Abstract

Background

Surgical reconstruction options of soft tissue defects include random pattern skin flaps. Flap survival depends on flap size and rotation arc and can be challenging regarding flap perfusion, leading to wound healing complications, insufficient wound coverage, and even to flap loss. Therefore, novel approaches that promote skin flap survival are required. Bone marrow-derived mesenchymal stem cells (MSCs) intravenous infusion is therapeutically efficient in various diseases via multimodal and orchestrated mechanisms, including anti-inflammatory, immunomodulatory effects, and via microvasculature re-establishment.

Methods

We used a modified McFarlane-type skin flap rodent model. After skin flap surgery, intravenous infusion of MSCs or vehicle was performed. *In vivo* optical near-infrared (NIR) imaging using indocyanine green was performed, followed by histological analysis, including hematoxylin and eosin (H&E), Masson's Trichrome (MT) staining, and gene expression analysis.

Results

The flap survival area was greater in the MSC group. *In vivo* optical NIR perfusion imaging analysis suggested that skin blood perfusion was greater in the MSC group. *Ex-vivo* histological analysis demonstrated that the skin structure was more clearly observed in the MSC group. The dermal thickness was greater in the MSC group, according to the MT staining results. We

observed a higher expression of FGF2 mRNA in the tissues of the MSC group using qRT-PCR.

Conclusions

These results suggest that intravenous infusion of bone marrow-derived MSCs promotes skin survival of random pattern flap, which is associated with an increased blood perfusion and a higher expression of FGF2 in a random skin flap rat model.

INTRODUCTION

In wound management, a set of levels of increasing complexity, referred to as the reconstructive ladder, is employed (1). The reconstructive ladder is a spectrum of closure options and the surgeon seeks the simplest or lower level on the ladder (1). In more severe wounds, the plastic and reconstructive surgeon may need to move up the ladder and utilize flap surgery, whereby the tissue from the donor is moved to another site. Plastic and reconstructive surgery advances have led to the development of various types of skin flaps (2). Random pattern flap is used to rescue complicated conditions (3). Different from the axial pattern flap, the random pattern flap contains no axial vessels and is nourished by the dermal, subdermal, or subcutaneous vascular network (3). Tissue ischemia in the random pattern flap can cause flap failure and lead to serious tissue necrosis, even though a surgical delay procedure is added to extend the flap survival (4, 5). Thus, the development of novel approaches to improve flap survival is important.

Intravenous infusion of bone marrow (BM)-derived mesenchymal stem cells (MSCs) is widely used to improve ischemic injury in central nervous tissues due to the multimodal and orchestrated therapeutic mechanisms of these cells, including anti-inflammatory and immunomodulatory effects, and re-establishment of the microvasculature (6-8). MSCs have also been applied to improve the survival of experimental random pattern skin flaps (9-15). Local injection of BM-derived (9, 12, 15) and adipose-derived MSCs (10, 11) increased the viability of random pattern skin flaps in rodent models. Intravenous infusion of adipose-derived MSCs has also increased skin flap

survival (13, 14). Intravenous application of bone marrow-derived MSCs is being used in several clinical studies and their safety has been validated (16).

Here, we asked whether intravenous infusion of adult BM-derived MSCs elicits an increased survival of random skin flap in rats.

MATERIALS AND METHODS

Animals

The use of animals was approved by the Animal Care and Use Committee of Sapporo Medical University, and all procedures were carried out in accordance with institutional guidelines. Male Wistar rats (n=66; 10 weeks old; weight 230 – 250 g) were used.

Preparation of MSCs from rat BM

Preparation and culture of MSCs were conducted based on our previous studies (8). Briefly, BM obtained from femoral bones of adult (6 – 8 weeks old) Wistar rats was diluted in 15 mL of Dulbecco's modified Eagle's medium (DMEM) (Sigma, St. Louis, MO, USA) supplemented with 10% heat-inactivated fetal bovine serum (Thermo Fisher Scientific Inc., Waltham, MA, USA), 2 mM L-glutamine (Sigma), 100 U/mL penicillin, and 0.1 mg/mL streptomycin (Thermo Fisher Scientific Inc.). Then, incubation for 3 days at 37ºC in a humidified atmosphere containing 5% CO_2 followed.

When a confluence state was almost reached, cells were detached using a trypsin-ethylenediaminetetraacetic acid solution (Sigma) and

subcultured at 1 × 10^4 cells/mL of medium. The MSCs after three passages were used in the present study. A previous phenotypic analysis of the surface antigens revealed cluster of differentiation (CD) 45^-, $CD73^+$, $CD90^+$, and $CD106^-$ on the MSCs (17).

Surgical Procedure

The animals were anesthetized using an intraperitoneal injection of ketamine (75 mg/kg) and xylazine (10 mg/kg). The back of the rats was shaved. Modified McFarlane-type caudally based skin flaps (3 × 8 cm) were used with a minor modification (18, 19). Briefly, the pedicles of flaps were set at the level of a horizontal line connecting the two iliac crests. The flaps were raised through the panniculus carnosus layer, not including the underlying fascia. All visible axial vessels were cauterized to ensure that the flaps were random-patterned. Then, the flaps were sutured back to their original position using 4-0 nylon monofilaments.

MSCs Infusion Procedure

The transplantation protocols differed between the 2 groups. One day after flap surgery, the animals were randomly divided into the MSC-treated group (n=24) and the vehicle group (n=24). The rats were intravenously infused with BM-derived MSCs (1.0 × 10^6 cells in 1 mL of fresh DMEM) or the vehicle alone (1 mL of fresh DMEM without MSCs) via the right femoral vein. We confirmed a high cell viability (> 99%) with 0.4% trypan blue, immediately after the procedure. Intact rats (n=18) were also used.

All rats were injected daily with cyclosporine A (10 mg/kg intraperitoneally) from one day before intravenous infusion (8, 20).

Flap Survival Analysis

Twenty-four-bit digital color images of the flaps at the same distance (14 cm) and using the same focus value were taken using a digital camera (DMC-LX3, Panasonic, Osaka, Japan) at days 0 and 14 after flap elevation surgery. The total areas of the flaps were traced and analyzed using ImageJ 2.0.0 (21). The survival area at day 14 compared to the total skin flap area at day 0 was calculated as the survival rate.

Histological Evaluations

After being photographed at day 14, the rats (n=6/group) were deeply anesthetized and the flap tissue was cut. A routine paraffin wax embedding procedure was performed. Briefly, the flap tissue samples were fixed in 4% paraformaldehyde in 0.1 M phosphate-buffered saline for 24 hours, dehydrated using a graded ethanol series, cleared in xylene, embedded in paraffin wax, and cut into 4-μm-thick sections. The tissue blocks were carefully chosen after histological assessment of the sections stained with H&E and MT. Images were acquired using a microscope (BZ-X710, Keyence Corp.). Computed quantification of the residual collagen (dermal collagen area) was performed at ± 2 mm around the borderline between the epidermis and the ulcer (green channel, threshold 31/255). The thickness of the proximal pedicle (yellow: Fig. 3B1, 3C1) and of the dermal collagen were measured at 0.5, 1.0, 1.5, and 2.0 mm distal to the borderline between the

epidermis and ulcer in each group (red line on dashed line: Fig. 3B, 3C). The survived dermal thickness ratio was calculated as follows: survived dermal thickness ratio = dermal collagen thickness at 0.5, 1.0, 1.5, and 2.0 mm distal to the borderline between the epidermis and ulcer/thickness of the proximal pedicle, respectively (Fig. 3B, 3C).

In vivo optical NIR perfusion imaging using indocyanine green (ICG)

At day 14, *in vivo* fluorescence imaging was performed using an IVIS Lumina Imaging System (Xenogen, Alameda, CA). The rats (n=10/group) were kept on the imaging stage under anesthetized conditions with 2.5% of isoflurane gas in an oxygen flow (1.5 L/min). Then, indocyanine green (ICG) (0.25 mg in saline) was injected into the tail vein. All images were acquired at 1 minute after ICG injection using the filter setting preset for ICG with a background, excitation, and emission wavelengths of 665 – 695, 710 – 760, and 810 – 875 nm, respectively. Consistent illumination parameters were used for all NIR fluorescent acquisitions: the field of view (FOV) was set at 12.5 cm, the exposure time was 2 s, f/stop value was 2, lamp voltage was set to “high,” and the binning was kept on “small”. All images were analyzed using the Living Image 3.2 software (Xenogen, Alameda, CA). The regions of interest (ROI) were caudally placed on the intact skin outside the flap (1 × 1 cm) as a control (green box). The distal end of the flap (2 × 1.5 cm) was considered as the distal area (blue box), and the area around the necrotic border zone (1 × 1.5 cm) was considered as the marginal area (yellow box). The photon ratio was defined as below: Photon ratio = total photon counts of target ROI/average photon counts of control ROI.

Quantitative reverse transcription-polymerase chain reaction

Animals (n=8/group) were sacrificed under deep anesthesia with ketamine (75 mg/kg, i.p.) and xylazine (10 mg/kg, i.p.), and the tissue samples (2 mm x 2 mm), were harvested from the flaps (4 cm from each pedicle). The tissue samples were stored at −80°C until further use. After homogenization, the total RNA was purified using the RNeasy Plus mini kit (QIAGEN, Venlo, the Netherlands). RNA quality was assessed using the Bioanalyzer RNA 6000 Nano kit (Agilent Technologies, Santa Clara, CA, USA). Samples with an RNA integrity number > 8.8 were used.

The Super Script® VILO™ cDNA Synthesis Kit (Invitrogen, Carlsbad, CA, USA) was used for reverse transcription. Total mRNA (~100 ng) was used for qRT-PCR analysis. TaqMan® Universal Master Mix II with Uracil-N glycosylase (UNG) and TaqMan® Gene Expression assays (Thermo Fisher Scientific Inc) were used. Specific sets of primers and TaqMan probes were purchased from Thermo Fisher Scientific Inc (FGF2: Rn00570809_m1 and GAPDH: Rn01775763_g1). qRT-PCR analysis was performed in triplicates using PRISM7500 and 7500 software v2.3 (Thermo Fisher Scientific Inc.). Thermal cycling was carried out at 50°C for 2 min and at 95°C for 10 min, followed by 40 cycles at 95°C for 15 s, and 60°C for 1 min. The delta cycle threshold (Ct) (ΔCt) was calculated against the endogenous control (glyceraldehyde 3-phosphate dehydrogenase), and the delta-delta Ct (ΔΔCt) was calculated against the ΔCt of the control. Fold change (FC) was also calculated using the comparative Ct method (22).

Statistical analysis

All statistical analyses were performed using EZR 1.41 for Windows (Saitama Medical Center, Jichi Medical University, Saitama, Japan), which is a graphical user interface for R (The R Foundation for Statistical Computing, Vienna, Austria), a modified version of R commander designed to add statistical functions frequently used in biostatistics. For multiple comparisons, we used one-way analysis of variance with Holm *post hoc* test and Kruskal-Wallis test with Holm post hoc test. Comparisons between two groups were performed using the student's *t*-test and Mann–Whitney *U*-test, respectively. A p value < 0.05 was considered statistically significant. All data are presented as mean ± SEM.

RESULTS

Skin flap survival

Macroscopic observation of the surgical site revealed that the total area of the skin flap was soft and covered with normal skin at day 0 (immediately after flap surgery). At day 14, the survival and necrotic regions were clearly demarcated on the flaps (vehicle: Fig. 1A1; MSC: Fig. 1B1). Necrotic eschars of the flaps were removed after flap excision and the survival areas were measured (vehicle: Fig. 1A2; MSC: Fig. 1B2). The green arrows indicate the borderline demarcation between the survival and necrotic areas on the skin flap. The survival area at day 14 was significantly greater in the MSC group

(Fig. 1B; n=16, 59.00 ± 1.98%) compared to the vehicle group (Fig. 1A; n=16, 42.87 ± 1.80%) (Fig. 1C; $p < 0.001$).

Histological evaluation of the skin flaps

H&E staining of the intact tissue demonstrated the normal structure of the skin, including the dermis and the skin appendages with no infiltration of inflammatory cells and no granulation tissue (Fig. 2A: intact). Although disruption of skin integrity at the distal side of the skin flap (green arrows) was observed in the vehicle (Fig. 2B) and MSC (Fig. 2C) groups, the dermis in the MSC group was more preserved with a milder disruption of skin's integrity, a lower loss of skin appendages, and lower inflammatory cell infiltration at the distal edge of the skin flap (Fig. 2C). The granulation tissue is also partially covered with epithelium in the MSC group. These suggest a re-epithelialization and a better wound healing (Fig. 2C). A much greater infiltration of neutrophils (purple cells) is observed in the vehicle group (Fig. 2B2), compared to the MSC group (Fig. 2C2).

MT staining of the intact tissue (Fig. 3A: intact) showed clear morphological features in normal skin, suggesting the possibility to identify the collagen in survival dermis and in the granulation tissue of the skin flap. The dermal collagen area in the MSC group (Fig. 3C: n=6; 3.18 ± 0.37 mm^2) was greater than in the vehicle group (Fig. 3B: n=6; 2.15 ± 0.20 mm^2) (Fig. 3D; $p < 0.05$). The thickness of the proximal pedicle was 1.50 ± 0.078 mm (n=6) in the vehicle group (yellow: Fig. 3B1) and 1.65 ± 0.108 mm (n=6) in the MSC group (yellow: Fig. 3C1). There were no statistical differences of the thickness of the proximal pedicle between the two groups. Quantitative analysis of dermal

collagen thickness at distances from the epithelium border (Fig. 3E) demonstrated that the MSC group was significantly thicker than the vehicle group at 0.5 mm ($p<0.05$), 1.0 mm ($p<0.05$), 1.5 mm ($p<0.05$), and 2.0 mm ($p<0.05$), respectively. These results indicate that intravenous infusion of BM-derived MSCs promotes the survival of severe ischemic skin lesions, which were shown in a random pattern flap rat model.

In vivo optical NIR perfusion imaging analysis

In vivo fluorescence imaging after ICG injection (Fig. 4A-C: n=10) showed that the photon ratio at the distal area (Fig. 4D) in the vehicle (1833 ± 151) and MSC group (2337 ± 162) is lower than in the intact group (3858 ± 98.6, $p < 0.001$). However, the photon ratio in the MSC group is greater than in the vehicle group ($p < 0.01$). The photon ratio at the marginal area (Fig. 4E) in the MSC group (2706 ± 137) is greater than that in the vehicle group (2126 ± 104, $p < 0.001$). These results provide further support that infused BM-derived MSCs protect skin blood perfusion in the random pattern flap rat model.

Gene expression

To investigate the expression level of FGF2 mRNA in the tissue (n=8/group), we performed quantitative RT-PCR (Fig. 5). Although qRT-PCR showed that the relative expression levels of FGF2 mRNA in the vehicle group (2.66 ± 0.36) were higher than those in the intact group ($p < 0.01$), the expression levels in the MSC group (5.88 ± 1.51) were highly elevated, compared with those in the vehicle group ($p < 0.05$). This result suggests that an increased

expression of FGF2 is associated with the promotion of random pattern flap survival.

DISCUSSION

We found that intravenous infusion of BM-derived MSCs promotes the survival of random pattern flaps in rats. The flap survival area in MSC-infused animals was significantly greater than that in the vehicle group. Histological analysis using H&E staining demonstrated that the preservation of the skin structure was clearly observed in the MSC group. The dermal collagen thickness, assessed using MT staining at several distances from the epithelium border, demonstrated that the dermis in the MSC group is significantly thicker than that in the vehicle group, suggesting that the development of a scar contracture would be reduced or prevented. *In vivo* optical NIR perfusion imaging analysis suggests that skin blood perfusion is preserved in the MSC group. We observed a significantly higher expression of FGF2 mRNA in the tissue from the MSC group using qRT-PCR. Thus, intravenous infusion of BM-derived MSCs promotes skin survival of random pattern flap through an increased blood flow and a higher expression of FGF2 in a random skin flap rat model.

Random pattern flap is not used as a reconstruction first choice, but as a later option, such as in the case of sequential flap failure. Its disadvantage is that an adequate blood supply could be highly limited to the area of the proximal pedicle. The degree of ischemia in the flap is generally worse in areas that are more distal to the pedicle. Thus, the skin deficit is mostly covered with a vascular-poor tissue in the distal area of the flap.

Infused MSCs might overcome this limitation by promoting skin survival of random pattern flaps. Here, we observed a possible re-epithelialization with a greater preservation of skin integrity, appendages, and granulation with epithelium, following MSC infusion. These extensions of the useful flap area might contribute to a better clinical outcome, i.e., even though partial necrosis is observed in the distal part of flaps, survival dermis or soft tissue could feed the skin grafts. These could also cover implants or fragile organs, and prevent severe scar contracture.

FGF2, also known as basic FGF (bFGF), is widely used in treating wounds and it activates multiple cells, including dermal fibroblasts, keratinocytes, and endothelial cells and can induce tissue remodeling, wound healing, and neovascularization (23). FGF2 expression level in the MSC group was higher than that in the vehicle group, which was higher than that in the intact group. However, this vehicle group increase appeared insufficient for facilitating an endogenous wound repair. Yet, infused MSCs elicited the promotion of extensive flap survival via increased expression levels of FGF2.

Regarding the angiogenic properties of FGF2, exogenous FGF2 stimulates the migration and proliferation of endothelial cells *in vivo*, and encourages mitogenesis of smooth muscle cells and fibroblasts, that induces the development of large collateral vessels with adventitia (24). Here, we observed an increased blood supply in both the distal and marginal areas of the skin flap evaluated using a NIR *in vivo* imaging system and a higher preservation of collagen thickness, which was assessed using MT staining. It is conceivable that an increased expression of FGF2 in the tissue might contribute to promoting the survival of the random pattern skin flap, following

intravenous infusion of BM MSCs.

Here, we employed modified McFarlane-type caudally based skin flaps (3 × 8 cm). In the original, the flap was raised by incision along three sides and completely elevated to its base at the level of the lower angles of the scapular (18). However, our pedicle is caudally based at the level of the posterior iliac crests (19) as an anatomical landmark, where there is less mobility than near the scapular. Thus, our skin flap was a useful experimental rat model for the quantification of the survival of skin areas.

A local injection of BM-derived MSCs has been applied to the random skin flap model, showing that these studies demonstrated an increased ischemic skin survival via neovascularization (9, 12, 15). However, the intravenous route has not been tested using BM-derived MSCs, whereas intravenous infusion of adipose-derived MSCs showed an increased survival area of the ischemic flap (13, 14). The underlying molecular mechanisms need to be further elucidated. The promotion of the survival area of the random skin flap, following intravenous infusion of BM-derived MSCs via the activation of FGF2 in the ischemic tissue, led to an increased blood supply and to greater wound healing. Further studies must be performed to elucidate the molecular pathways regarding FGF2 in this model system using intravenous infusion of BM-derived MSCs.

CONCLUSIONS

Intravenous infusion of BM-derived MSCs might impact the survival of random pattern skin flaps via an increased microvasculature, leading to an increased blood supply and to an FGF2 upregulation.

Acknowledgments

This work was supported in part by the funding for education and research at Sapporo Medical University and RR&D Service of Department of Veterans Affairs (B7335R, B9260L).

Figure legends

Figure 1

Photographs of random pattern skin flaps in the vehicle infused group (A1) and MSC infused group (B1) at day 14 postoperatively. Necrotic eschars were removed in the vehicle group (A2) and MSC group (B2) for measurement of the flap survival area (C). Green arrows indicate the borderline of demarcation between survived and necrotic areas on the skin flap. Asterisks indicate *** $p < 0.001$ using Mann-Whitney *U* test. Scale bars = 10 mm.

Figure 2

Photomicrograph of H&E staining stained skin flap section in intact (A), vehicle (B) and MSC (C) infused groups at day 14 postoperatively. Green arrows indicate the same borderline at Fig. 1, indicating the demarcation between the survived and necrotic areas on the skin flap. High-power microscopic images (A2, B2, C2) are taken from asterisks (A1, B1, C1), respectively. Scale bars = 1 mm (A1, B1, C1), 200 μm (A2, B2, C2).

Figure 3

Photomicrograph of Masson's Trichrome stained skin flap section in intact (A), vehicle (B) and MSC (C) infused groups at day 14 postoperatively. Green arrows in B1 and C1 indicate the same borderline at Fig. 1 indicating the demarcation between the survived and necrotic areas on the skin flap. Quantification of residual collagen (Student's *t*-test) (D). Dermal collagen thickness (Mann-Whitney *U* test) (E). Yellow arrows in B1 and C1 indicate

proximal pedicles. High-power microscopic images (A2, B2, C2) are taken from asterisks (A1, B1, C1), respectively. Scale bars = 1 mm (A1, B1, C1), 200 μm (A2, B2, C2). Asterisks indicate *p < 0.05.

Figure 4

In vivo fluorescence imaging after indocyanine green injection in intact (A), vehicle (B), and MSC (C) infused group at day 14 postoperatively. For quantification of photon counts, three regions of interest (ROI) were placed as the control area (green boxes), marginal area (yellow boxes), and distal area (blue boxes). Quantification of photon ratio at the distal area (Kruskal-Wallis test with Holm post hoc test) (D) and marginal area (Mann–Whitney *U*-test) (E). Scale bars = 10 mm. Asterisks indicate **p < 0.01, ***p < 0.001.

Figure 5

mRNA expression of FGF2. Quantitative reverse transcription polymerase chain reaction (qRT-PCR) data of FGF2 is shown. Intact, vehicle, and MSC groups were used. The Y-axis shows the $2^{-\Delta\Delta Ct}$ of mRNA gene expression. Asterisks indicate *p < 0.05, ***p < 0.001 using one-way analysis of variance with Holm *post hoc* test.

References

1. Boyce, D. E., Shokrollahi, K. Reconstructive surgery. *BMJ (Clinical research ed)* 2006;332:710-712.

2. Hashimoto, I., Abe, Y., Ishida, S., et al. Development of Skin Flaps for Reconstructive Surgery: Random Pattern Flap to Perforator Flap. *J Med Invest* 2016;63:159-162.

3. Zheng, H.-P., Xu, Y.-Q., Lin, J., Hu, D.-Q. Development History of Flap. *Atlas of Perforator Flap and Wound Healing: Microsurgical Reconstruction and Cases*. Singapore: Springer Singapore; 2019:3-10.

4. Morrow, B. T. Plastic Surgery Techniques for Wound Coverage. *Surg Clin North Am* 2020;100:733-740.

5. Acartürk, T. O., Dinçyürek, H., Dağlıoğlu, K. Delay by Staged Elevation of Flaps and Importance of Inclusion of the Perforator Artery. *J Hand Microsurg* 2015;7:1-5.

6. Sasaki, M., Oka, S., Kataoka-Sasaki, Y., Kocsis, J. D., Honmou, O. "Chronic" State in Neural Diseases as the Target of Cellular Therapy with Mesenchymal Stem Cells. *World Neurosurg* 2020;135:375-376.

7. Nakazaki, M., Oka, S., Sasaki, M., et al. Prevention of neointimal hyperplasia induced by an endovascular stent via intravenous infusion of mesenchymal stem cells. *J Neurosurg* 2019:1-13.

8. Nakazaki, M., Sasaki, M., Kataoka-Sasaki, Y., et al. Intravenous infusion of mesenchymal stem cells improves impaired cognitive function in a cerebral small vessel disease model. *Neuroscience* 2019;408:361-377.

9. Chehelcheraghi, F., Abbaszadeh, A., Tavafi, M. Skin Mast Cell Promotion in Random Skin Flaps in Rats using Bone Marrow Mesenchymal Stem Cells and Amniotic Membrane. *Iran Biomed J* 2018;22:322-330.

10. Foroglou, P., Demiri, E., Koliakos, G., Karathanasis, V. Autologous administration of adipose stromal cells improves skin flap survival through neovascularization: An experimental study. *Int Wound J* 2019;16:1471-1476.

11. Izmirli, H. H., Alagoz, M. S., Gercek, H., et al. Use of Adipose-Derived Mesenchymal Stem Cells to Accelerate Neovascularization in Interpolation Flaps. *J Craniofac Surg* 2016;27:264-271.

12. Kira, T., Omokawa, S., Akahane, M., et al. Effectiveness of Bone Marrow Stromal Cell Sheets in Maintaining Random-Pattern Skin Flaps in an Experimental Animal Model. *Plast Reconstr Surg* 2015;136:624e-632e.

13. Lee, D. W., Jeon, Y. R., Cho, E. J., Kang, J. H., Lew, D. H. Optimal administration routes for adipose-derived stem cells therapy in ischaemic flaps. *J Tissue Eng Regen Med* 2014;8:596-603.

14. Suartz, C. V., Gaiba, S., Franca, J. P., Aloise, A. C., Ferreira, L. M. Adipose-derived stem cells (ADSC) in the viability of a random pattern dorsal skin flap in rats. *Acta Cir Bras* 2014;29 Suppl 3:2-5.

15. Zheng, Y., Yi, C., Xia, W., et al. Mesenchymal stem cells transduced by vascular endothelial growth factor gene for ischemic random skin flaps. *Plast Reconstr Surg* 2008;121:59-69.

16. Honmou, O., Onodera, R., Sasaki, M., Waxman, S. G., Kocsis, J. D. Mesenchymal stem cells: therapeutic outlook for stroke. *Trends Mol Med* 2012;18:292-297.

17. Kim, S., Honmou, O., Kato, K., et al. Neural differentiation potential of peripheral blood- and bone-marrow-derived precursor cells. *Brain Res* 2006;1123:27-33.

18. McFarlane, R. M., Deyoung, G., Henry, R. A. THE DESIGN OF A PEDICLE FLAP IN THE RAT TO STUDY NECROSIS AND ITS PREVENTION. *Plast Reconstr Surg* 1965;35:177-182.

19. Rinker, B., Fink, B. F., Barry, N. G., Fife, J. A., Milan, M. E. The effect of calcium channel blockers on smoking-induced skin flap necrosis. *Plast Reconstr Surg* 2010;125:866-871.

20. Sasaki, M., Radtke, C., Tan, A. M., et al. BDNF-hypersecreting human mesenchymal stem cells promote functional recovery, axonal sprouting, and protection of corticospinal neurons after spinal cord injury. *J Neurosci* 2009;29:14932-14941.

21. Rueden, C. T., Schindelin, J., Hiner, M. C., et al. ImageJ2: ImageJ for the next generation of scientific image data. *BMC Bioinformatics* 2017;18:529.

22. Schmittgen, T. D., Livak, K. J. Analyzing real-time PCR data by the comparative C(T) method. *Nat Protoc* 2008;3:1101-1108.

23. Akita, S., Akino, K., Hirano, A. Basic Fibroblast Growth Factor in Scarless Wound Healing. *Adv Wound Care (New Rochelle)* 2013;2:44-49.

24. Beenken, A., Mohammadi, M. The FGF family: biology, pathophysiology and therapy. *Nature Reviews Drug Discovery* 2009;8:235-253.

Figure 1

Click here to access/download;Figure;Nakagawa_Figure1.TIF

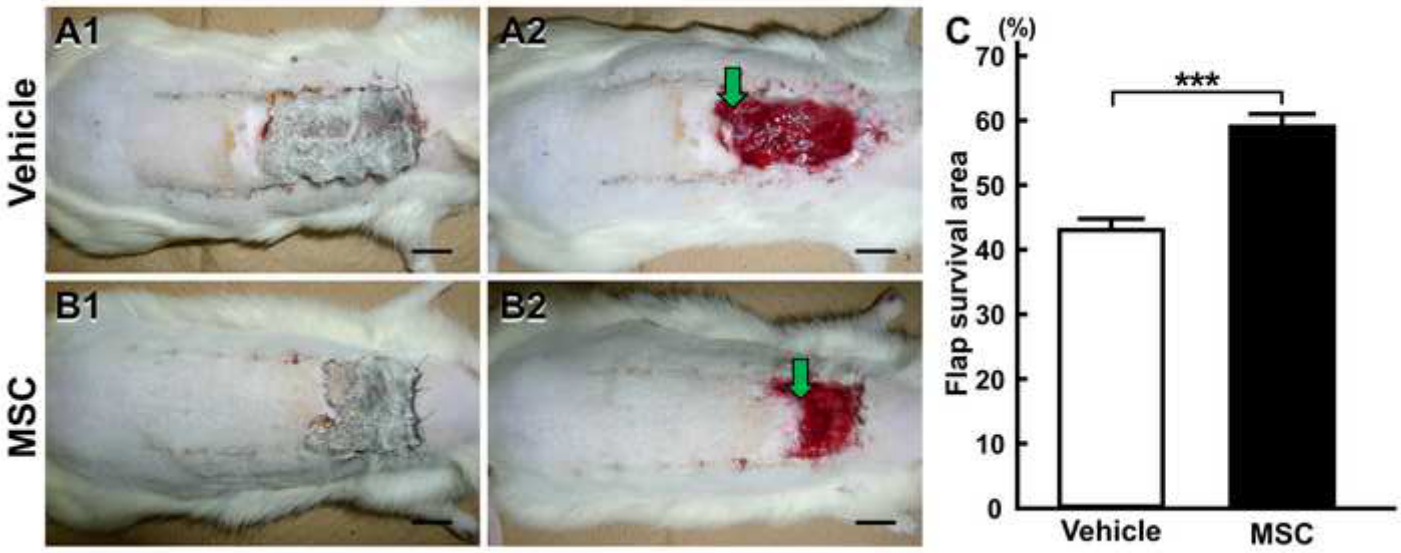

Figure 2

Click here to access/download;Figure;Nakagawa_Figure2.TIF

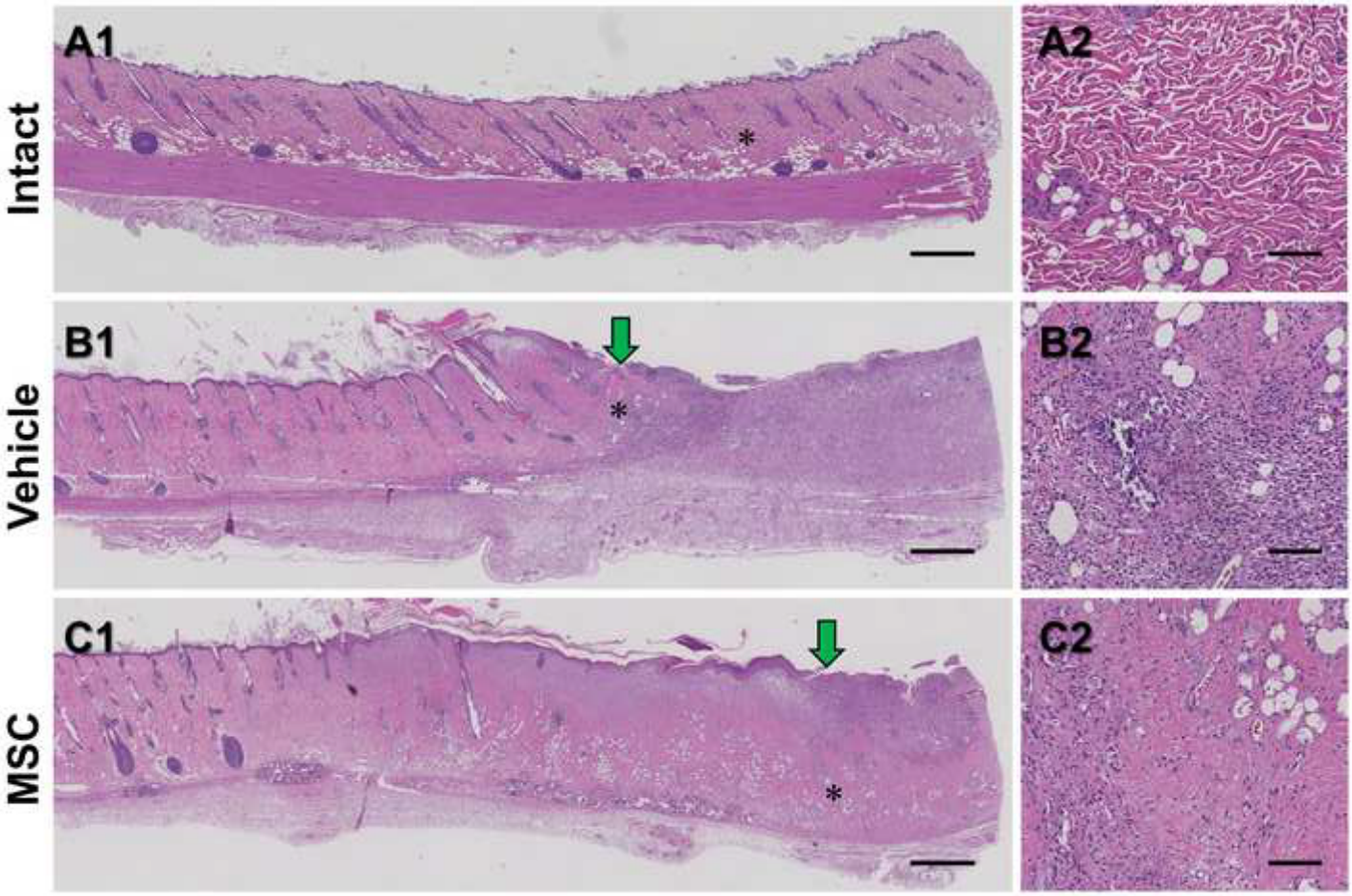

Figure 3

Click here to access/download;Figure;Nakagawa_Figure3.TIF

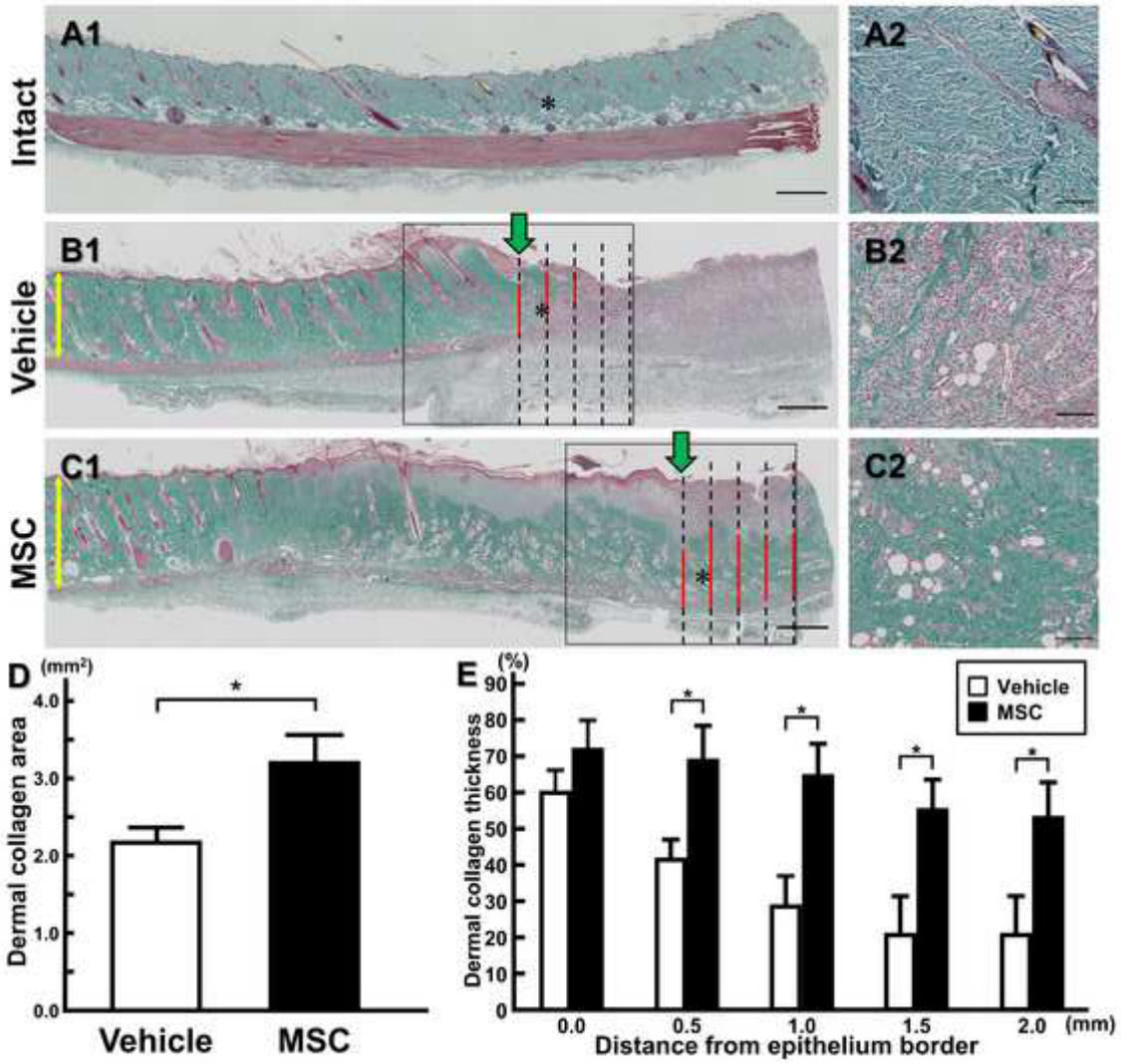

Figure 4

Click here to access/download;Figure;Nakagawa_Figure4.TIF

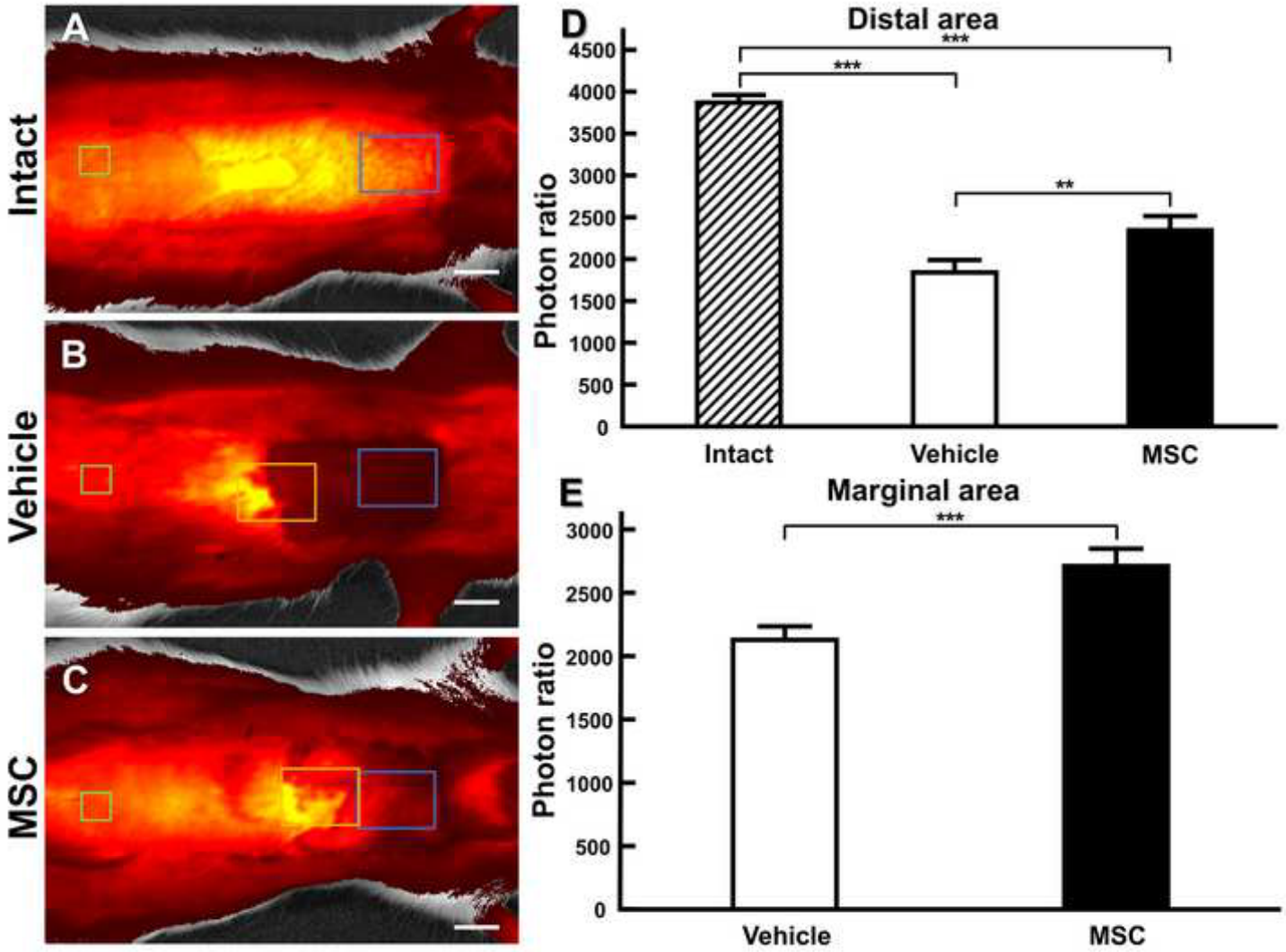

Figure 5

Click here to access/download;Figure;Nakagawa_Figure5.TIF